BY DR. SLOBODAN CUK,
President, TESLAco

Part 3

Single–Stage Bridgeless Isolated PFC Converter Achieves 98% Efficiency

A new Single-stage AC-DC Converter achieves Power Factor Correction (PFC) and isolation (patents pending). This converter operates directly from the ac line, eliminating a Full-bridge Rectifier needed in conventional PFC converters, which require at least two, but most often three processing stages to achieve isolation.

Until now, it was considered impossible to have an AC-DC converter with PFC and isolation features provided in a single power processing stage and without mandatory full-bridge rectifier. This is not the case anymore. The high performance of the non-isolated Bridgeless PFC converter (described in July 2010 *Power Electronics Technology*) with 0.999 Power Factor and 1.7%THD harmonic distortion is preserved with the only addition being an appropriately inserted isolation transformer. An Integrated Magnetics extension results in a single magnetic component, 3-switch configuration, compared to 14-switches and four magnetic components of the conventional Three-stage approach. As a result, this Single-stage solution has much improved efficiency of over 98%, compared to 90% of the Three-stage approach and offers simultaneously significant size and cost reductions.

The first limitation is found in the conventional Boost PFC converter shown in *Fig. 1a*, which can operate only from the rectified ac line as illustrated by the waveforms in *Fig. 1b*, thus resulting in two-stage power processing. An additional problem is that there is no simple and effective way to introduce the isolation in the conventional Boost converter of Fig. 1a.

As seen in *Fig. 2a*, one approach is to use a full-bridge extension of the Boost converter to introduce isolation, which is then controlled as PFC converter. Note, however, its complexity consisting of four transistors on the primary side and four diode rectifiers on the secondary side operating at the switching frequency of, for example, 100kHz with additional four diodes of input bridge rectifier operating at the line frequency of 50Hz or 60Hz resulting in total 12 switches. The line current will then have the superimposed input inductor ripple current at high switching frequency, which needs to be filtered out by an additional high frequency filter on ac line. The presence of 12 switches and their operation in the hard-switching mode results in high conduction and switching losses. The best efficiency reported with this two-stage approach is 87%, which also included additional switching devices to achieve resonant transitions and reduce switching losses.

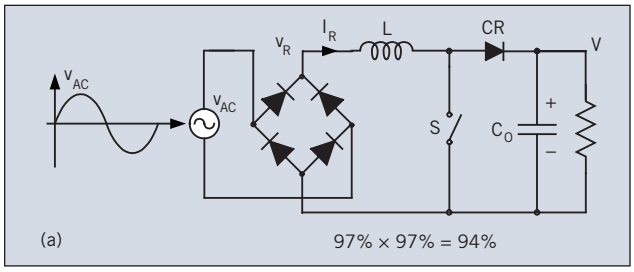

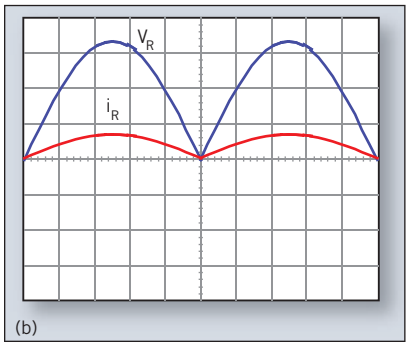

Fig. 1a. A full-bridge diode rectifier together with boost converter used as a two-stage solution for non-isolated AC-to-DC power conversion with Power Factor Correction feature. 1b. Waveforms of the rectified line voltage and current in the PFC converter of Fig. 1a.

This configuration has the start-up problem occurring due to step-up only DC voltage gain. Thus, additional circuitry is needed to pre-charge the output capacitor before start up of the converter. This problem does not exist in the Isolated Bridgeless PFC converter as described in later sections.

The most common approach for 1 kW or higher power, however, is to use a Three-stage power processing illustrated in *Fig. 3a*, in which the Bridge Rectifier on input is followed by the isolated full-bridge Boost PFC converter. In this case, a

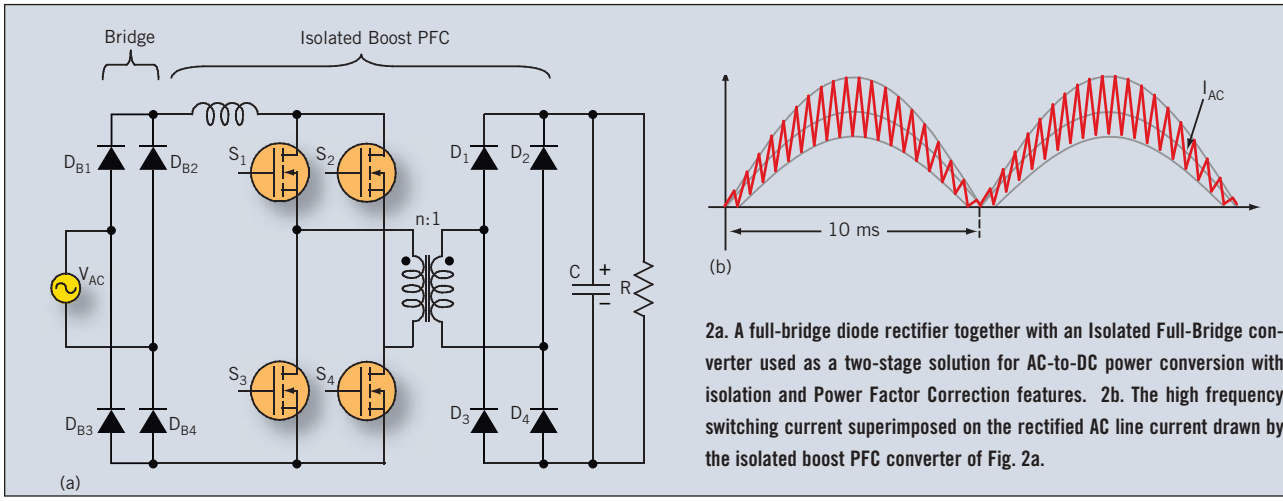

2a. A full-bridge diode rectifier together with an Isolated Full-Bridge converter used as a two-stage solution for AC-to-DC power conversion with isolation and Power Factor Correction features. 2b. The high frequency switching current superimposed on the rectified AC line current drawn by the isolated boost PFC converter of Fig. 2a.

total of fourteen (14) switches is needed! The highest efficiency is up to 90%, so it is better then the two-stage approach. Therefore, this three-stage approach is utilized in practically all present applications for high power.

For medium and low power, an alternative approach with reduced number of switches is shown in *Fig. 3b*, in which the forward converter was used for the isolation stage. While the number of switches is reduced to ten, the problem is that four switching devices in the forward converter are still exposed to much increased voltage stresses on both primary side switches and secondary side switches when compared to the two-stage full-bridge solution. Note also that four magnetic pieces must be used as in full-bridge solution, when a input filter inductor is included.

NEW ISOLATED BRIDGELESS PFC CONVERTER

Clearly, the present AC-to-DC solutions with PFC and isolation use a configuration with three cascaded converters (bridge rectifier followed by two DC/DC converters) so that total power is processed in sequence three times, resulting in high power losses and low overall efficiency.

The Bridgeless PFC converter in *Fig. 4a* and its duty ratio modulation control of *Fig. 4b* were shown in July's *Power Electronics Technology* to operate directly from the ac line and without the need

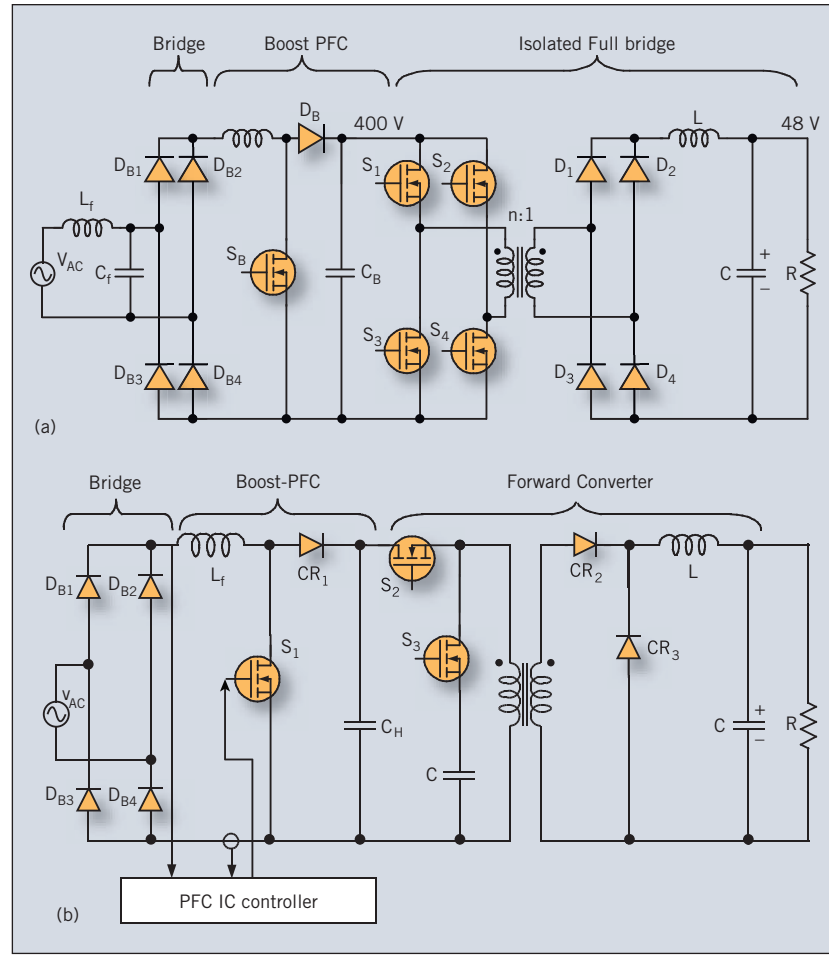

Fig. 3a. A full-bridge diode rectifier followed by boost PFC converter and an Isolated Full-Bridge converter used as a Three-stage solution for AC-to-DC power conversion with isolation and Power Factor Correction comprises 14 switches and 4 magnetic components.

Fig. 3b. A full-bridge diode rectifier followed by boost PFC converter and an isolated forward converter used as a Three-stage solution for AC-to-DC power conversion with isolation and Power Factor Correction features comprises 10 switches and 4 magnetic components, when an input filter inductor is included.

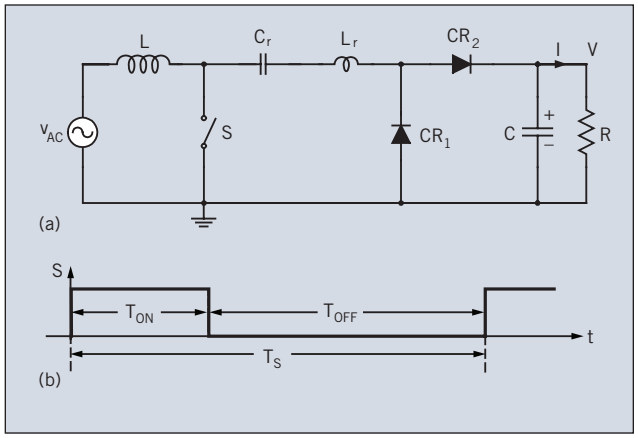

Fig. 4a. A Bridgeless PFC Converter topology with a single controllable switch S. Fig. 4b. States of a single controllable switch S in the Bridgeless PFC Converter of Fig. 4a.

for the Full-Bridge rectifier in front. This converter has only three switches and operates on the basis of the new hybrid- switching method. Despite the use of a resonant inductor and a resonant capacitor, this hybrid switching method results in the DC voltage gain being dependent on the duty ratio only and having the same DC voltage gain as the ordinary boost converter for either positive input voltage or negative input voltage, hence providing an automatic ac line rectification without the need for a front-end bridge rectifier.

The clear objective now becomes to introduce the isolation to the Bridgeless PFC converter in the simplest and most efficient way. The desired way would be not to increase the number of switches (as it was needed for ordinary boost converter!) and to obtain the simple and efficient isolation transformer. Both objectives are achieved by following a simple procedure outlined in the sequence of equivalent circuit transformations illustrated in *Figs. 5a, 5b* and *5c*. Note that in these equivalent circuits the input voltage is designated as a positive DC source Vg in order to simplify the designation of respective components in steady-state conditions. The actual ac-dc converter is powered by the time varying ac source Vg(t).

First, the resonant capacitor is split into two resonant capacitors Cr1 and Cr2 connected in series as illustrated in *Fig. 5a*. Then, an inductor with magnetizing inductance, Lm is connected from their common connection point A to ground G as illustrated in *Fig. 5b*. Since now there are two capacitors, each one will settle on its own DC voltages V1 and V2 respectively. We can find these voltages using the State-Space Averaging, or volt-second balance on the two inductors L and L_m. However, a faster way is to use some circuit shortcuts. For example, the loop consisting of input source, two inductors L and L_m and resonant capacitor Cr1 must satisfy the requirement that the summation

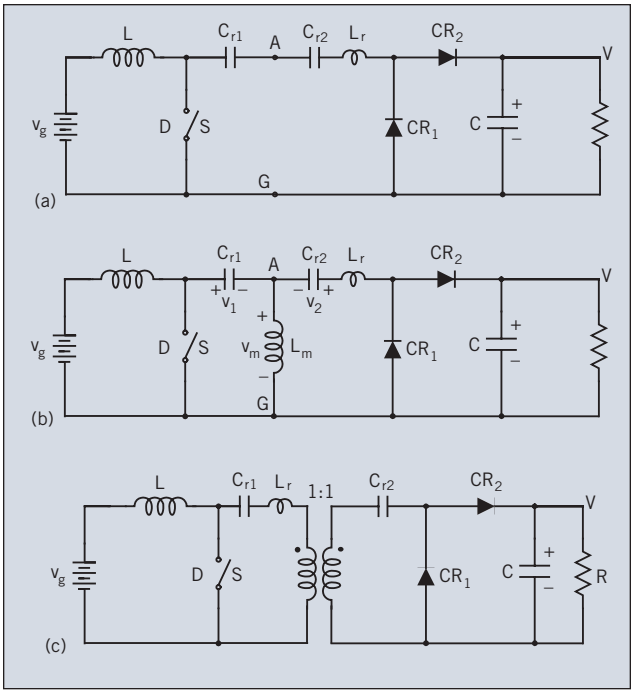

Fig. 5a-c. Step-by-step procedure of how to introduce the isolation transformer into the non-isolated Bridgeless PFC converter of Fig. 4a.

of DC voltages around the loop must be equal to zero. However, since neither inductor can support net average voltage across it, their DC voltage contributions are zero resulting that resonant capacitors Cr1 voltage V1 must be equal to input source voltage Vg and of the polarity as shown in *Fig. 5b*. On the other hand, during the ON-time interval, the two resonant capacitors are placed in parallel across the magnetizing inductance L_m, which imposes that the DC voltage V2 of resonant capacitor Cr2 must be equal to voltage V1, or:

$$V_1 = V_2 = V_g \qquad (1)$$

Now one can calculate the voltage across the magnetizing inductance L_m during the OFF-time interval as:

$$Vm\ (OFF\text{-}time) = V - Vg = D/(1-D)\ Vg \qquad (2)$$

Since output DC voltage was not changed by the above equivalent circuit transformations and is equal to:

$$V = V_g / (1-D). \qquad (3)$$

This proves that the magnetizing inductance Lm is automatically volt-second balanced for any operating duty ratio D. Therefore, one can replace this magnetizing inductance with a 1:1 turns ratio two winding transformer

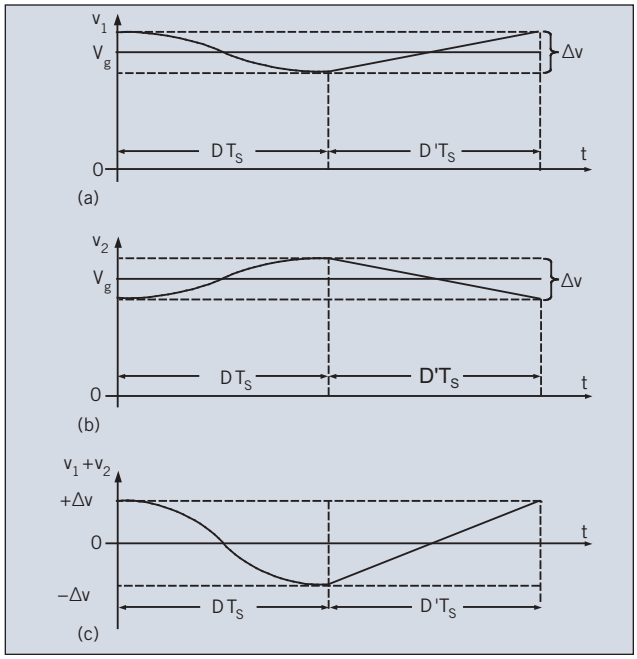

Fig. 6a-c. The salient waveforms of the converter in Fig. 5c: a) voltage waveform on the primary side resonant capacitor Cr1 b) voltage waveform on the secondary side resonant capacitor Cr2 c) ripple voltage waveform equal to the sum of the ripple voltage waveforms on both resonant capacitors Cr1 and Cr2.

as illustrated in *Fig. 5c*.

The actual time domain voltage waveforms on the two resonant capacitors are shown in *Fig. 6a* and *Fig. 6b* to have the same DC voltage Vg but superimposed on that DC voltage are the two ripple voltages which are out of phase, since during the OFF-time interval first resonant capacitor Cr1 is charging while the second resonant capacitor Cr2 is discharging and opposite taking place during the ON-time interval. Therefore, the resulting net ripple voltage across the series capacitors is equal to twice the ripple voltage on each capacitor and has no net DC voltage as shown by the waveform in *Fig. 6c*.

Note also that during the ON-time interval, the equivalent circuit as shown in *Fig. 7a* is obtained. As the magnetizing inductance Lm is large, and its impedance is very large so, to the first order, this impedance is not loading the circuit in *Fig. 7a* and can be removed from it to result in the resonant circuit model as in *Fig. 7b* in which the equivalent resonant capacitor Cr can be calculated from:

$$1/C_r = 1/C_{r1} + 1/C_{r2} \qquad (4)$$

Therefore, the same resonant current waveforms as previously obtained for the non-isolated converter of *Fig. 4a* and respective analytical results apply directly to the isolated converter.

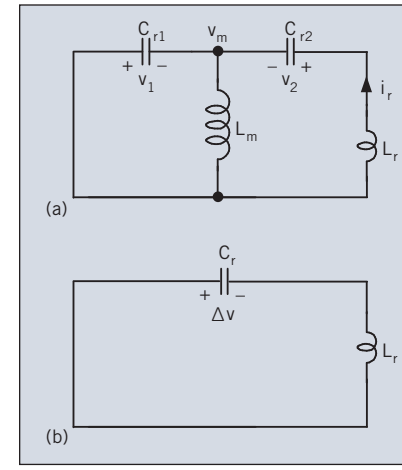

Fig. 7a. The equivalent resonant circuit model of converter in Fig. 5b, and Fig. 7b is simplified resonant circuit model of circuit in Fig. 7a.

Note that the above analysis proceeds in the same way for the negative input voltage. Even though the steady-state conditions on the two resonant capacitors Cr1 and Cr2 will now appropriately change including the voltage polarity on them, the same output DC voltage gain given by (3) will remain. Therefore, the goal stated at the very beginning of inserting the isolation transformer into the non-isolated converter structure with minimum disturbance so that its original operation can be maintained is achieved: the isolated configuration has the same three-switch configuration, with a single controlling switch on the primary now, and two passive diode switches on the secondary side.

Now one can scale the transformer turns ratio from 1:1 to transformer with primary Np turns and secondary Ns turns as shown in *Fig. 8a* and result in overall DC voltage

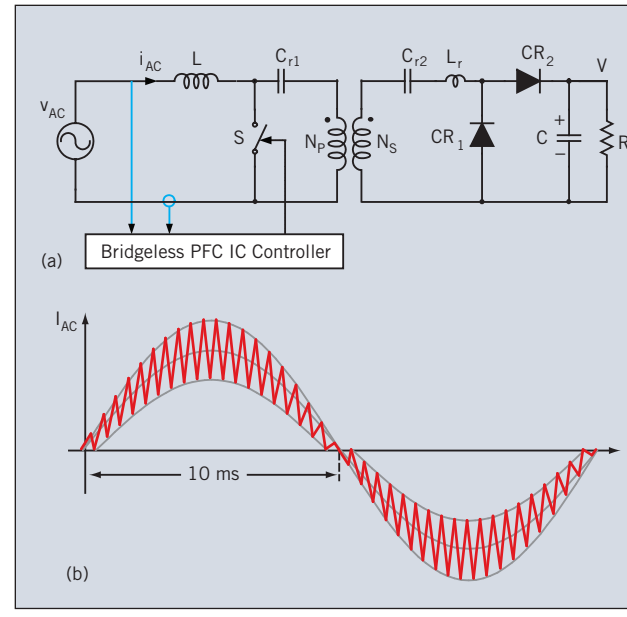

Fig. 8a. An Isolated Bridgeless PFC Converter topology with a single controllable switch S controlled by Bridgeless PFC IC chip. 8b. The high frequency switching current superimposed on the 50Hz input AC line current drawn by the Isolated Bridgeless PFC converter of Fig. 8a.

ratio of

$$V/V_g = N_S / N_P \; 1/(1\text{-}D) \qquad (5)$$

In addition to isolation, this gives an added flexibility so that the output voltage can be via turns ratio scaled down to any desired output DC voltage.

Note that the Bridgeless PFC IC Controller is now on the primary side of the converter as illustrated in *Fig. 8a*, which will result in the line current waveform as shown in *Fig. 8b* which has a high frequency input inductor ripple (at the switching frequency of 50kHz for example) superimposed on the low frequency (50Hz) line current. The high switching frequency ripple current is then filtered out by use of a separate high frequency filter on the converter input.

ISOLATION TRANSFORMER ADVANTAGES

The procedure followed to introduce the isolation transformer described above also highlights some of the key advantages of this transformer compared to isolation transformer in conventional isolated converters such as, for example, the forward converter and the flyback converter, as illustrated by the B-H loop curve of their respective transformers shown in *Fig. 9*.

First, the isolation transformer of the forward converter uses only one half of the available B-H loop as the transformer flux is set in one direction by the input switch and input voltage source, but also requires a reset mechanism to return the flux to original zero AC flux position. The reset mechanism involves either a third reset winding or more commonly used a flyback type reset, known as a voltage clamp reset in forward converter.

The isolation transformer in flyback converter also uses only one half of the core flux capability as forward converter. However, it has an additional drawback that its transformer during ON-time stores all the input energy and during OFF-time releases stored energy to the load. Therefore, the flyback-type transformer must use a large air-gap to store that energy resulting in much reduced

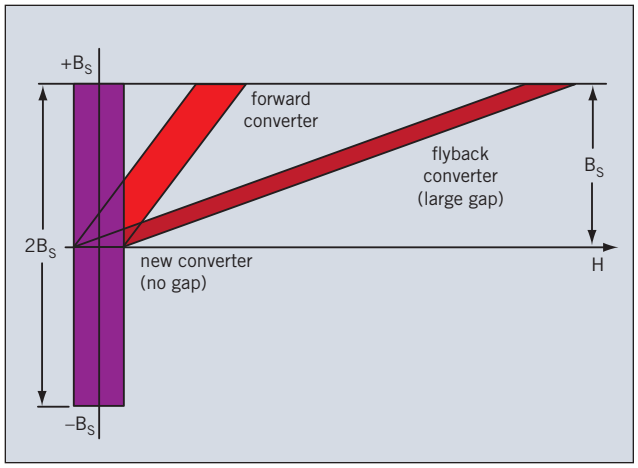

Fig. 9. A comparison of the operating B-H loop characteristics of the three isolation transformer types used in: a) Isolated Bridgeless PFC converter b) forward converter c) flyback converter.

magnetizing inductance as illustrated by the reduced slope of the B-H loop. The larger the dc load current the smaller is this slope. The ac flux is then superimposed on top of this large dc bias, leaving only a remaining available flux density for the AC flux.

The isolation transformer in the Isolated Bridgeless PFC converter utilizes both parts of the available core flux capability as illustrated in Fig. 9. In addition there is no need for third reset winding or voltage clamp type of reset as in forward converter as the transformer is automatically volt-second balanced for any duty ratio D. In addition, this transformer operates as a true ac transformer as it does not store DC energy and can therefore be built on an un-gapped magnetic core resulting in large magnetizing inductance and small magnetizing current. The fact that this isolation transformer does not store any DC energy like a flyback converter can be easily verified on the converter itself: the primary winding has in series with it a primary side resonant capacitor Cr1 which must be charge balanced and the same holds true for the secondary side resonant capacitor Cr2. Therefore,

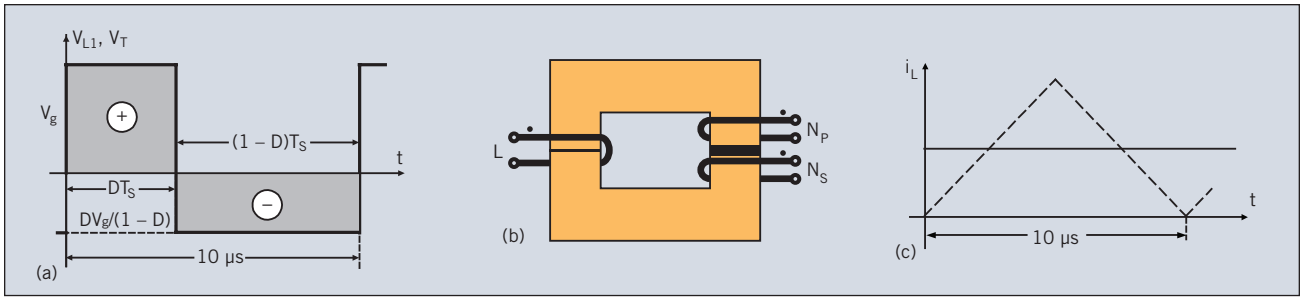

Fig. 10a. The identical voltage waveforms on inductor L and transformer t_{out} of the converter in Fig. 8a, 10b. The integration of the transformer and inductor onto the common magnetic core to produce an integrated magnetic structure. 10c. The resulting zero input ripple current obtained by implementation of Integrated Magnetics structure of Fig. 10b.

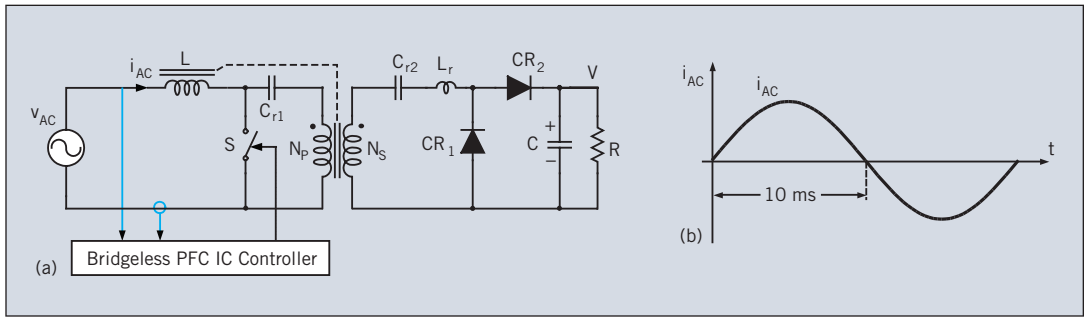

Fig. 11a. An Integrated-Magnetics Bridgeless PFC Converter with a single switch S controlled by Bridgeless PFC IC chip.

Fig. 11b. The 50Hz input AC line current drawn by the Integrated-Magnetics Isolated Bridgeless PFC converter of Fig. 11a.

neither primary nor secondary winding can have a net DC current, so the transformer itself does not store any energy.

These isolation transformer advantages clearly translate into a much smaller size and higher efficiency of the transformer, which has bi-directional flux capability with no DC energy storage.

The converter of Fig. 8a has two magnetic pieces: the input inductor and the isolation transformer requiring two magnetic cores. However, the converter topology of Fig. 8a has a unique property: both inductor L and transformer primary t_{out} have the identical square-wave excitation voltages vL1 and Vp for any operating duty ratio D as illustrated in *Fig. 10a*. In the loop consisting of primary winding of the isolation transformer and input voltage source, the ac model is obtained by shorting the input voltage source and primary resonant capacitor resulting in the inductor winding and transformer primary winding being in parallel across each other. Therefore, regardless of the ac voltage excitations, both inductor and transformer have identical ac waveforms which makes it possible to place them on the common

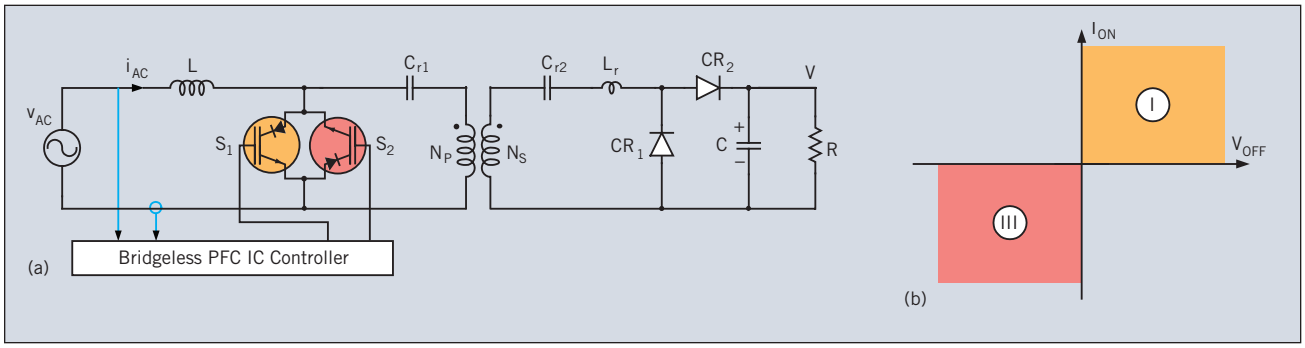

Fig. 12a The Isolated Bridgeless PFC converter with implementation of switch S with two RBIGBT devices connected in parallel. Fig. 12b. The two-qaudrant requirements imposed on switch S operating in the first and third quadrant.

core, as shown in *Fig. 10b*, thus eliminating one magnetic core. Furthermore, the proper placement of the air-gap on the common core, such as on the side of the transformer (Fig. 10b) shifts all the ripple current from the inductor winding into transformer winding, resulting in zero ripple current of the input inductor current as illustrated with full line in *Fig. 10c*. Thus, the converter could even operate on the boundary of the Discontinuous Inductor Current Mode (DICM) as shown by the dotted line current waveforms in Fig. 10c, and still result in a very small near zero input inductor ripple current.

Clearly, such a large inductor ripple current would require a substantial separate high frequency filter in the conventional three-stage approach. Here it comes literally with no penalty, but in fact with additional size and performance advantages. For example, such large allowed input inductor ripple current could be used to reduce the size of the Integrated Magnetics core. Furthermore, operation at the edge of DICM was shown in the past to result in low total harmonic distortion for line frequency of 400Hz. Such Integrated Magnetic implementation is shown in *Fig. 11a* and respective clean ac line free of high frequency harmonics in *Fig. 11b*.

The current direction in the resonant inductor is changing from one direction in OFF-time interval to another direction in ON-time interval. This change of the direction of inductor current during the short transition could cause the voltage spikes on the switch S. The faster the change, the bigger the voltage spike would be. However, due to small energy stored in this small inductor, this spike can be effectively suppressed by use of a Zener diode, which would limit the voltage spike and dissipate its energy. Since the converter operates for both polarities of the input voltage, the bi-directional Zener diode, called Transorber, is used in practical application. This, once again, would dissipate all of the voltage spike energy and limit the spike voltage. However, a number of non-dissipative ways also can be employed to recover most of the energy contained and deliver it to the load, thus increasing the efficiency and reducing switch stresses during the transition.

IMPLEMENTING CONTROLLABLE SWITCH S

As shown before for the nonisolated Bridgeless PFC converter (July Power Electronics Technology), the same implementations for switch S equally applies for this Isolated Bridgeless PFC converter: two RBIGBTs in converter of *Fig. 12a* and two n-channel MOSFETs in converter of *Fig. 16a*.

It is expected that a single two-quadrant switch having the characteristics of *Fig. 12b* will be available soon. As the conduction losses are by far the dominant losses of the Isolated Bridgeless PFC Converter, such two-quadrant switch implementation would raise the overall efficiency from the current 97% to over 98%.

The low voltage stresses of the switches in the Isolated Bridgeless PFC Converter of *Fig. 13a* are shown in *Fig.*

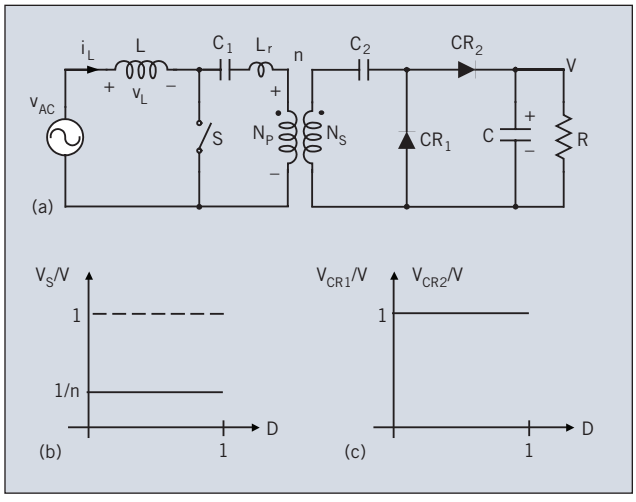

Fig. 13a. The Isolated Bridgeless PFC converter with n:1 turns ratio of the isolation transformer. Fig. 13b. The voltage stress on the single controlled switch S is equal to output voltage scaled by transformer turns ratio.

Fig. 13c. The voltage stress on the two secondary side current rectifiers is equal to the output voltage.

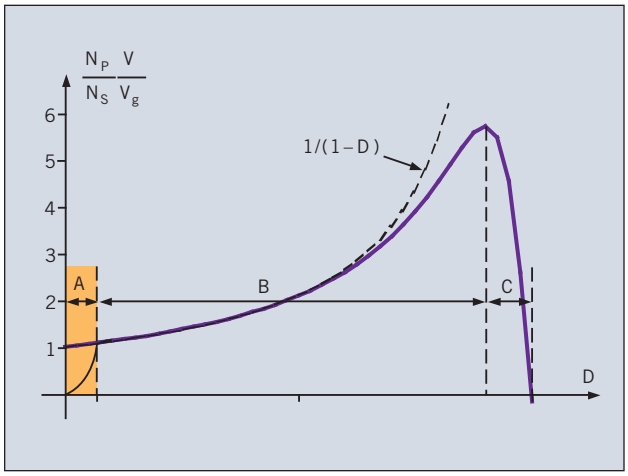

Fig. 14. Start-up operation: Measured dc voltage gain characteristic exhibits the step-down gain characteristic at very low duty ratios as shown by shaded region, allowing for a soft star-up and eliminating the need for a separate circuit to charge the output capacitor required in conventional boost -type converters.

13b for primary switch S and in *Fig. 13c* for secondary side rectifiers CR1 and CR2. The secondary side current rectifiers have the voltage stresses equal to the output DC voltage and therefore result in minimum voltage stress. The voltage stress of the input switch S is also low since it is equal to the output voltage reflected by the turn's ratio of the transformer. Low voltage stresses lead to higher efficiency and converter cost reduction.

The DC gain characteristic of Isolated Bridgeless PFC Converter of (5) suggests the start-up problem for the same reason as the other isolated boost converters, such as one in *Fig. 2a* having the same boost type gain characteristic (5). This converter, however, does not have such a start-up problem due to its special mode of operation at low duty ratios, which permit a soft-start from zero output voltage.

Shown in *Fig. 14* with dashed line is the ideal dc voltage gain characteristic given by Equation (5) for the special case of 1:1 isolation transformer, which was used in experimental verification. Just as in the non-isolated Bridgeless PFC Converter, the actual measured dc voltage gain shown in solid line reveals the existence of the shaded region at very low duty ratios during which the dc conversion gain drops to zero. Therefore, effectively, the actual measured dc voltage gain is that of a step-down/step-up type. Thus, the output dc voltage can be started smoothly from zero dc output voltage and brought by duty ratio increase into a step-up dc conversion region, without the need for separate start-up circuitry to pre-charge the output capacitor to the DC voltage gain of one as would be otherwise needed.

The insertion of the isolation transformer demonstrated

TABLE		
POWER PROCESSING	**SINGLE-STAGE**	**THREE-STAGE**
Type of Converter	**ISOLATED BRIDGELESS PFC**	**BRIDGE-BOOST PFC-FULL-BRIDGE**
Switching Method	HYBRID	Square-wave
Number of switches	3	14
Transistors	1	5
Switch-voltage Stress	Low	High
Lossless-switching	YES	NO
Control	Simple	Complex
Magnetics pieces	1	4
Power Losses	2%	10%
Efficiency	>98%	88% to 90%
Size	Small	Big
Weight	Light	Heavy
Cost	Low	High

Table: Comparison of the Single-stage solution of Isolated Bridgeless PFC converter with a Three-stage approach of Bridge rectifier, Boost PFC converter and an Isolated Full-Bridge Converter.

that the original topological structure and PFC performance of the Bridgeless PFC converter (nonisolated) is preserved in the isolated extension including retaining the same switches. Therefore, the original converter prototype of 400W of the Bridgeless PFC converter (August *Power Electronics Technology*) was modified by inserting a 1:1 isolation transformer. As expected, the power factor (PF) and Total Harmonic Distortion (THD) measurements remain the same at 0.999 PF and 1.7%THD for 60Hz, 110V line operation.

However, the efficiency was reduced by the losses in the added isolation transformer, resulting in an added power loss of 0.25% to 0.5% depending on the size of the transformer.

Besides the large number of switches it requires, the conventional Three-stage conversion also results in large voltage stresses on some of the switches, as it uses an intermediate 400V high voltage DC bus. The conceptual diagram shown in *Fig. 15a* indicates these three conversion stages and the conversion step-up to intermediate 400V high DC voltage bus.

The single-stage conversion of the Isolated Bridgeless PFC Converter eliminates the intermediate high DC voltage bus goes directly from the AC line through built-in rectification and PFC conversion to isolated lower voltages such as 48V used in telecommunication shown *Fig. 15b*.

The comparison of the key performance characteristics of the Single-stage Isolated Bridgeless PFC converter with the conventional Three-stage approach using the Bridge Rectifier, Boost PFC converter and Isolated Full-Bridge Converter is shown in the *table*.

Note in particular the dramatic reduction of the number of switches from 14 to 3 and simultaneous efficiency improvement from 90% to over 97% with the magnetic components reduction from 4 to 1 and corresponding large reduction in weight, size and cost.

Hybrid switching has made possible the use of Single-stage approach and isolation transformer insertion with minimum change from the operation of the non-isolated version.

Several applications of the Isolated Bridgeless PFC Converter confirm the converter's versatility for a wide power range from 75W to several kilowatts.

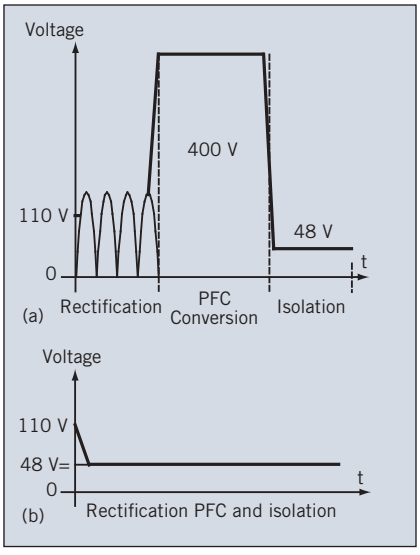

Fig. 15a. A Three-stage power processing with the voltage rectification and then step-up voltage conversion to intermediate 400V DC line used as an input for the isolated step-down voltage conversion for the converter of Fig. 3b. 15b. A Single-stage direct step-down conversion to the output DC voltage without the intermediate high DC bus voltage and yet providing isolation and PFC features.

BUILT-IN ADAPTER FOR LAPTOP COMPUTERS

Past attempts to put AC Adapters inside laptop computers have failed for two reasons:

1. Low efficiency below 90% causes too much dissipation, even at 75W.
2. Large size due to many magnetic pieces, which do not fit within the low profile of laptop computers.

Both of these problems are now resolved with the Isolated Bridgeless PFC converter, which can be designed to provide for example, 100W laptop AC adapter generating 18V to 20V DC output and charging the laptop battery directly from the ac line while providing unity power factor and low distortion.

Furthermore, a single Integrated Magnetic piece can be made using the flat magnetic core, thus meeting the low profile requirements of even most demanding current laptop computers with the low profile of less than one inch. Finally, to increase efficiency, the output diode rectifiers can be implemented with two synchronous rectifier MOSFETs and high-side drivers, such as illustrated in *Fig. 16a*. To further reduce size and cost, two MOSFETs and high side drivers could be replaced by a single integrated silicon solution, such as Dr MOS, available from a number of semiconductor vendors.

BATTERY CHARGER FOR HYBRID CARS AND ELECTRIC BICYCLES

Another attractive application is a battery charger for hybrid and electric cars (*Fig. 16b)*, which is used to charge 200V Lithium Ion batteries used in most hybrid cars. Clearly, the high efficiency will result in increased miles traveled per cost of charge.

Electric bicycles are becoming more popular worldwide, especially in Japan and Europe. At present, there are no portable chargers for bicycles due to their current large size. The new Isolated Bridgeless PFC converter can be used for 120W portable chargers for bicycles and eliminate the need for big, bulky and costly home charger.

Finally, for industrial applications, more efficient, smaller, and less expensive battery chargers for forklift trucks, golf carts, and wheelchairs will be available.

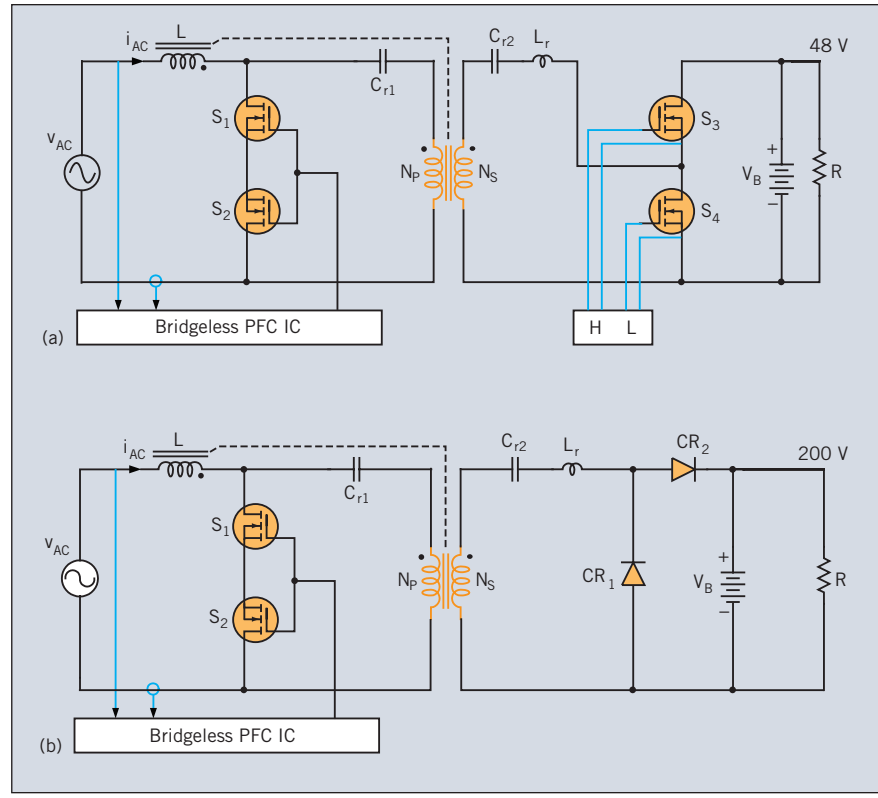

Fig. 16a shows the Isolated Bridgeless PFC converter of Fig. 13a with implementation of two MOSFETs on the secondary side controlled by high-side driver control chip, which are suitable for 18V built-in AC adapter designs and 48V telecommunication supply. Fig. 16b Isolated Bridgeless PFC converter with implementation of switch S with two back-to-back MOSFET devices operating in the first and third quadrant, suitable for 200V hybrid car charger.

TELECOMMUNICATIONS POWER SUPPLY

As the telecommunications power has standardized on 48V battery as a back-up source for its reliable operation, the Isolated Bridgeless PFC converter fits into that application as well as it can provide a low-cost and efficient rectifier for the 3kW and 10kW needed in those applications.

The new Hybrid Switching method has enabled the Single-stage Isolated Bridgeless PFC Converter, which consists of only three switches and one magnetic component, to effectively replace a Three-stage approach with up to 14 switches and 4 magnetic components. The resultant large reduction of losses and simultaneous reduction of size, weight, and cost, suits this approach to a host of consumer and industrial applications.

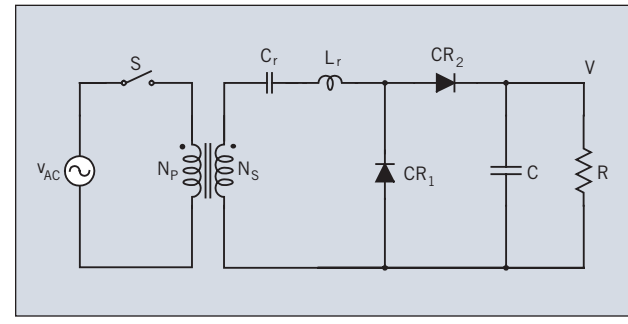

Fig. 17. Third "impossible" converter solution: Isolated Bridgeless PFC converter with pulsating input current.

THIRD "IMPOSSIBLE" CONVERTER SOLUTION

The third in a series of "impossible" converter solutions, the "Isolated Bridgeless PFC Converter with Pulsating Input Current" (patents pending), is shown in *Fig. 17*. The converter has a transformer with flyback-type characteristics, yet its output DC voltage is positive (not negative as in flyback converter) and its DC voltage gain characteristic is of the boost type, that is 1/(1-D).

Footnote: Isolated Bridgeless PFC Converter™ and Single-stage Isolated PFC Converter™ are trademarks of TESLAco.

Editorial Note: For questions regarding this article and for contact information to the author the readers are directed to TESLAco's Web site www.teslaco.com.

REFERENCES

1. Slobodan Cuk, "Modelling, Analysis and Design of Switching Converters", PhD thesis, November 1976, California Institute of Technology, Pasadena, California, USA.

2.. Slobodan Cuk, R.D. Middlebrook, "Advances in Switched-Mode Power Conversion, " Vol. 1, II, and III, TESLAco 1981 and 1983.